



# Implantable Sensor System for Remote Detection of a Restenosis Condition

J. A. Miguel, Y. Lechuga, R. Mozuelos, M. Martínez

## ► To cite this version:

J. A. Miguel, Y. Lechuga, R. Mozuelos, M. Martínez. Implantable Sensor System for Remote Detection of a Restenosis Condition. 4th Doctoral Conference on Computing, Electrical and Industrial Systems (DoCEIS), Apr 2013, Costa de Caparica, Portugal. pp.164-171, 10.1007/978-3-642-37291-9\_18 . hal-01348747

**HAL Id: hal-01348747**

**<https://hal.science/hal-01348747>**

Submitted on 25 Jul 2016

**HAL** is a multi-disciplinary open access archive for the deposit and dissemination of scientific research documents, whether they are published or not. The documents may come from teaching and research institutions in France or abroad, or from public or private research centers.

L'archive ouverte pluridisciplinaire **HAL**, est destinée au dépôt et à la diffusion de documents scientifiques de niveau recherche, publiés ou non, émanant des établissements d'enseignement et de recherche français ou étrangers, des laboratoires publics ou privés.



Distributed under a Creative Commons Attribution 4.0 International License

# Implantable Sensor System for Remote Detection of a Restenosis Condition

J. A. Miguel, Y. Lechuga, R. Mozuelos and M. Martínez

Microelectronics Engineering Group  
University of Cantabria Av. de los Castros s/n  
39005 Santander, Spain  
{joseangel.miguel, yolanda.lechuga, roman.mozuelos, mar.martinez}@unican.es

**Abstract.** The increase of life expectancy in the European Union, and the high risk of cardiovascular diseases associated with age, are some of the main factors to contribute to the rise of healthcare costs. An intelligent stent (e-stent), capable of obtaining and transmitting real-time measurements of physiological parameters for its clinical consultation, can be a useful tool for long-term monitoring, diagnostic, and early warning system for arterial blockage without patient hospitalization. In this paper, a behavioural model of capacitive Micro-Electro-Mechanical (MEMS) pressure sensor is proposed and simulated under several restenosis conditions. Special attention has been given to the need of an accurate fault model, obtained from realistic finite-element simulations, to ensure long-term reliability; particularly for those faults whose behavior cannot be easily described by an analytical model.

**Keywords:** Biomedical Electronics, Implantable Biomedical Devices, Biomedical Transducers, Cardiology, MEMS Testing, Fault Injection.

## 1 Introduction

Cardiovascular diseases are the leading cause of mortality in the European Union (EU), being responsible of nearly 35% of all deaths in the year 2009 [1]. Percutaneous Coronary Interventions (PCIs) are the most common coronary revascularization procedures, consisting mainly of a balloon angioplasty procedure with stent placement. A stent is a bio-compatible mesh tube designed to be inserted into the body in a collapsed way, mounted at the tip of a catheter with a deflated balloon inside it. At the point of blockage of a blood vessel, the balloon is inflated, so the stent is expanded against the vessel walls, where it is deployed in order to create a durable unobstructed path for blood flow.

The stent has had a strong impact in modern cardiovascular medicine, positioning as a minimally invasive alternative to coronary artery bypass grafting surgery (CABG), with a short recovery time and low major complications rate. Particularly, the University Hospital Marqués de Valdecilla in Santander (Spain) conducts more than 1500 procedures with stent implantation per year. Unfortunately, this procedure is not exempt of long-term complications as the in-stent restenosis (ISR), that consists of

the re-occlusion of the vessel lumen due to physiological repair mechanisms triggered by damage induced to the vessel walls during an angioplasty procedure [2].

The development of MEMS, together with micro-fabrication technologies compatible with CMOS fabrication processes, allow the integration of sensor structures and electronic circuits in the same chip, increasing the capabilities of implantable medical electronic devices. An intelligent stent (e-stent) that incorporates a sensor and integrated electronic circuitry, capable of monitoring and transmitting real-time measurements of physiological parameters related to blood vessel occlusion, such as pressure and flow velocity, can be a useful tool to ISR early detection [3-5].

It is relevant to point out that an implantable sensor must fulfil certain design restrictions, including reduced size, low power consumption, low cost, and above all, long-term reliability and stability. This is why heterogeneous testing, fault modelling and fault injection are critical issues to validate the fabricated device.

In this paper an initial model of a proposed ISR monitoring device is presented and evaluated under different grades of stenosis; focusing on the analysis of MEMS pressure sensors, to estimate the influence of their most common fabrication faults on the system response. Section II summarizes the relationship of this work to the Internet of Things (IoT). Section III describes the behavioural model of the proposed implantable device under different grades of stenosis. In Section IV analytical models of a MEMS pressure sensor are validated using FEM simulations. A common fabrication fault error is injected into the FEM model, so that its influence on the sensor response can be quantified. The paper finishes in Section V with the conclusions and future work.

## 2 Relationship to the Internet of Things

The Internet of Things (IoT) was born with the main objective of providing wireless communication capabilities to daily life objects, in order to create a new network concept based on the interaction between an imaginary environment (internet) and the real world (objects and sensors). The application of IoT technology in the healthcare field represents a potential way to minimize, social problems related, among others, to population aging and the associated risk of long-term diseases.

In this sense, a field of interest in the IoT lies in the concept of Medical Body Area Networks (MBAN) [6]. The use of implantable or wearable sensors, together with the addition of network connectivity, short range wireless communication to handheld modules, and remote data transmission via mobile phone or home gateway, can optimize the way medical data is nowadays acquired, stored and analyzed by healthcare providers. This type of sensors offers numerous benefits, such as continuous monitoring of patient's health state and personalized treatment or instantaneous first aid notification in the case of critical condition

This work proposes a behavioural model of an implantable pressure sensing device for the pulmonary artery, capable of obtaining and transmitting real-time measurements for the early detection of ISR condition without patient hospitalization.

### 3 Intelligent Stent Model

Blood flow and pressure measurements are some of the most commonly carried out procedures to monitor cardiovascular diseases. In this field, three approaches have been proved to be compatible with e-stent design: electromagnetic, ultrasonic and pressure-based techniques [3-5]. Pressure-based techniques are of special interest, because of their simple implementation, low power requirements, reduced dimensions and integration capabilities of sensors and electronic circuits on the same silicon substrate. Moreover, these approaches allow measuring both blood flow velocity and pressure in the vessel, providing a complete set of data to carry out ISR follow-up. The relationship between the two physiological parameters in an obstructed vessel can be expressed as [7]:

$$\Delta P = R_1 \cdot v + R_2 \cdot v^2 + R_3 \cdot \frac{dv}{dt} \quad (1)$$

Where  $\Delta P$  is the pressure gradient between both sides of the stenosis,  $v$  is the mean cross-sectional flow velocity in the vessel, and  $R_1$ ,  $R_2$  and  $R_3$  are coefficients that depend on the geometry of the obstruction and fluid properties. Parameter  $R_3$  is related to fluid inertial effects and has been reported to be despicable under medium to strong stenosis conditions [7].

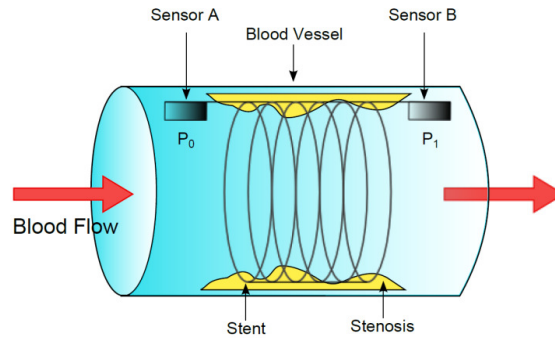


**Fig. 1.** Sensor placement and measures.

The simplest pressure-based e-stent implementation consists of a pair of capacitive MEMS sensors to measure blood pressure and an inductance to form an LC tank for remote power transfer and data transmission through inductive coupling. Fig. 1 shows a simplified representation of the proposed device, where  $P_0$  and  $P_1$  are blood pressure values in the heart and distal sides of the stent respectively.

A behavioural model of the implantable device, implemented in Matlab, is shown in Fig.2. This model has been simulated under different grades of stenosis, by varying  $R_1$  and  $R_2$  parameters, in order to obtain an approximation of its response under real disease conditions.

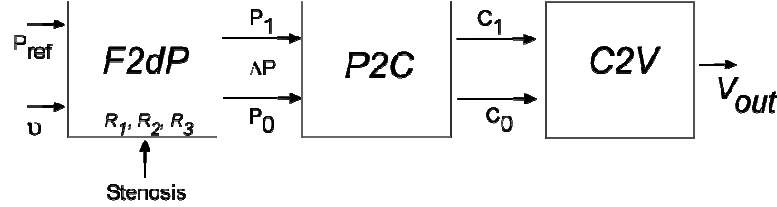


Fig. 2. Simplified model of the electronic system.

The first block of the model, called F2dP, converts blood flow velocity to differential blood pressure in the pulmonary artery, using the relationship exposed in (1). The values of  $R_1$  and  $R_2$  have been taken from clinical trials concerning ISR [8], as seen in Table 1. Using pressure and blood flow velocity signals from clinical trials, the F2dP block provides two pressure waveforms to be measured by the proximal ( $P_0$ ) and distal ( $P_1$ ) MEMS sensors.

**Table 1.** Characteristics of the instantaneous flow velocity and pressure gradient relationship.

Condition	R1	R2
Normal artery	$0.032 \pm 0.018$	$0.00030 \pm 0.0049$
Intermediate stenosis	$0.15 \pm 0.11$	$0.0021 \pm 0.0014$
Severe stenosis	$2.67 \pm 1.58$	$0.0014 \pm 0.010$

The P2C block contains an analytical model of a capacitive MEMS pressure sensor. This kind of sensor consists of a fully clamped diaphragm suspended over a sealed cavity and a fixed backplate. Once a uniformly distributed pressure is applied to the sensor, the top membrane deforms towards the backplate, reducing the chamber size and causing an increase in the resulting capacitance. A more detailed sensor description will be carried out in section IV.

The C2V block converts the output capacitance value from the pressure sensors to electric digital voltage signals  $V_0$  and  $V_1$ . The former voltage is related to the pressure recorded at the proximal location of the stent, while the latter is proportional to the pressure at the distal side. The converter model presents a linear response; and its description has been selected to be similar to common capacitance-to-digital converters (CDC) [9]. The most relevant parameters of the model are: a reference capacitance of 1.5 pF, a conversion range of 1.7 pF and a resolution of 10 bits. Moreover, several undesired effects, such as capacitive input noise, absolute error after calibration, gain error, integral nonlinearity and differential nonlinearity, have been taken into account to obtain a first estimation of their influence over the pressure and flow velocity measurements.

The behaviour of the modelled system for low ISR rate in the pulmonary artery is shown in Fig. 3. It shows the output voltage of the system (right graph), as a function of the blood flow signal for a healthy artery, and pressure waveforms to be measured by the MEMS sensors (left graph).

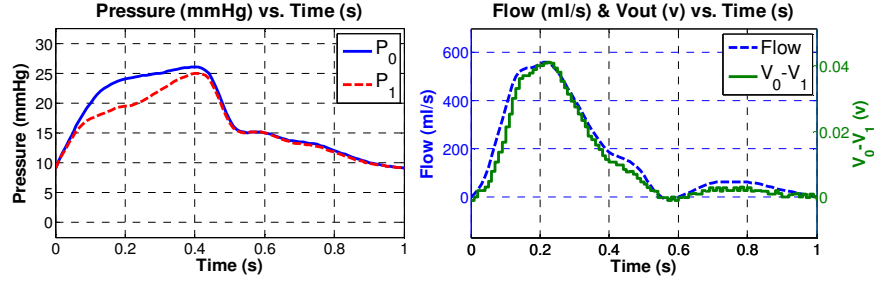


Fig. 3. Output system voltage compared to blood flow (right), reflecting the differential pressure measured in a pulmonary artery under low stenosis conditions (left).

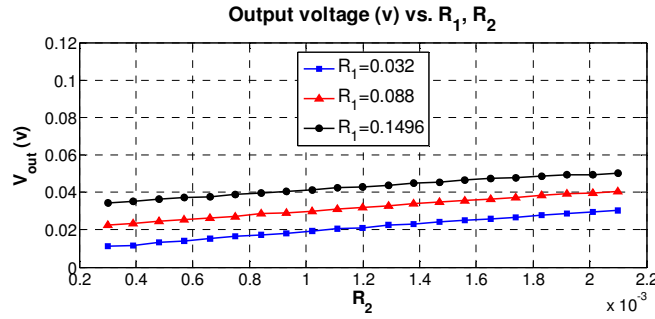


Fig. 4. Output mean voltage for  $R_1$  and  $R_2$  parameter sweep.

Several sets of  $R_1$  and  $R_2$  parameters have been introduced in the model, to generate blood flow waveforms under various real ISR conditions. As shown in Fig. 4, worse ISR conditions, reflected in higher  $R_1$  and  $R_2$  values, increase the pressure gradient along the longitudinal axis of the e-stent, as well as the mean output voltage of the system. The simulation results show a similar behaviour to the one expected (1), and have been compared to experimental data obtained from clinical trials [10].

It must be noted that a fault-free analytical model of the sensor has been used to carry out the previous simulations. As will be seen in the next section the accuracy of the mathematical models under faulty conditions must be analyzed, in order to evaluate its influence in the behaviour of the whole device.

#### 4 Capacitive MEMS Pressure Sensor

The principle of operation of MEMS capacitive pressure sensor is based on the concept of a two parallel plate capacitor, as mentioned in Section III. Fig. 5 shows a typical cross-sectional view of this kind of sensors, where  $P$  is a uniformly distributed pressure applied to the sensor,  $w_0$  is the center deflection of the membrane,  $t_g$  is the gap between the membrane and the fixed backplate when the external pressure is equal to the one in the cavity, and  $t_m$  is the thickness of the diaphragm.

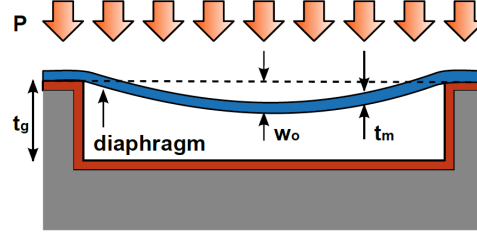


Fig. 5. Output mean voltage for  $R_1$  and  $R_2$  parameter sweep.

The deflection of a fully clamped circular diaphragm can be analytically modeled as a function of the radial distance from the center of the plate [11]. To validate this approach, some assumptions must be considered [11]: (a) the material of the diaphragm must have isotropic mechanical characteristics; (b) the thickness of the metallic electrode on the plate has to be neglected; (c) the gap between the plates needs to be small compared to the lateral extents of the plates, so the electric field fringing effects can be depicted; (d) the residual stresses in the diaphragm are not considered. Once fulfilled the previous requirements, the deflection of a circular diaphragm under large deflection conditions ( $w_0 > 30\% t_m$ ) can be stated as:

$$w(r) = w_0 \cdot \left[ 1 - \left( \frac{r}{a} \right)^2 \right]^2. \quad (2)$$

$$w_0 = \frac{3Pa(1 - \nu^2)}{16Et_m^3} \cdot \frac{1}{1 + \frac{0.488w_0^2}{t_m^2}}. \quad (3)$$

Where  $r$  is the distance to the center of the diaphragm,  $a$  is the radius of the diaphragm, and  $w_0$  is the maximum center deflection.

Once known the expression relating radial displacement and pressure applied to a fully clamped circular diaphragm, the sensor capacitance can be defined as:

$$C = \iint_A \frac{\epsilon_0 r dr d\theta}{t_g - w(r)} = \frac{\epsilon_0 A}{t_g} \sqrt{\frac{t_g}{w_0}} \tanh^{-1} \left( \sqrt{\frac{w_0}{t_g}} \right) = C_0 \sqrt{\frac{t_g}{w_0}} \tanh^{-1} \left( \sqrt{\frac{w_0}{t_g}} \right). \quad (4)$$

Where  $C_0$  is the capacitance of the undeflected sensor,  $\epsilon_0$  is the dielectric permittivity of free space, and  $A$  is the common area of the plates.

Finite element analysis (FEA) techniques allow non-linear mechanical and electromagnetic simulations of complex structures. In the particular case of MEMS pressure sensors, FEA analysis enables the validation of the aforementioned analytical models under various environmental conditions, as well as fault injection in the structural model of the sensor. Fig.6 shows the analytical and FEA capacitance and deflection response of a pressure sensor with a polysilicon diaphragm (Young Modulus:  $E = 169$  GPa; Poisson Ratio Coefficient:  $\nu = 0.22$ ) of  $4\mu\text{m}$  thickness, a radius of  $350\mu\text{m}$  and a sealed cavity of  $2\mu\text{m}$  height.

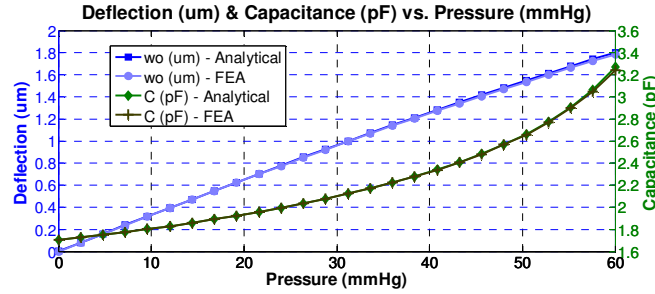


Fig. 6. Output mean voltage for  $R_1$  and  $R_2$  parameter sweep.

Because of its small thickness and high deformation degree, the sensor's diaphragm can be considered to be the most vulnerable part to fabrication defects. As the critical element of a capacitive sensor, its analytical model response, obtained from (2), (3) and (4), has been compared to the one from a FEA simulation, in fault injection cases. Fig. 7 contains analytical and FEA results when a defect, in the form of a pyramidal protuberance, appears on the top diaphragm of the sensor. This type of defect has been reported to occur because of the presence of impurities during the anisotropic wet etching of a single crystal silicon; a widely used process to create membranes [12]. Fig. 7 (left) shows that the capacitance response of the sensor, under constant pressure conditions, decreases for higher pyramid base areas at the center of the diaphragm. Fig. 7 (right) contains the capacitance results, under similar pressure conditions, calculated for different locations of a pyramid with a base side of  $50\mu\text{m}$ .

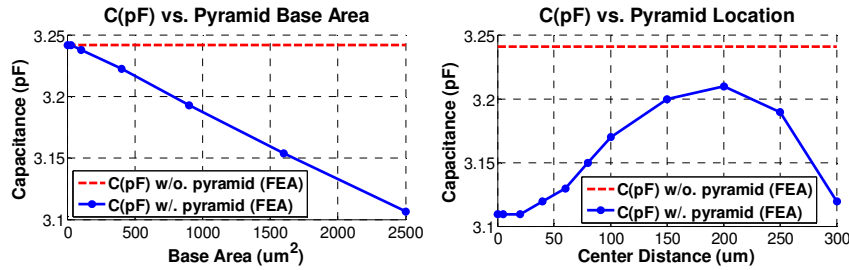


Fig. 7. Capacitance for different pyramid base sizes (*left*) and capacitance for different pyramid locations from the center of the diaphragm (*right*), under a pressure of 8kPa.

As shown in Fig. 7, the presence of a pyramid on the top membrane of the sensor reduces its deflection and equivalent output capacitance value, implying a loss of sensor sensitivity which can seriously compromise its reliability.

As shown in Fig. 6, an acceptable analytical solution can be achieved in the fault-free case, based on (2), (3) and (4). However, this mathematical formulation is no longer valid for modeling a faulty membrane. Hence, it is necessary to create additional analytical membrane models under faulty conditions, considering deflections results obtained from FEA simulations; especially for those faulty cases in which the geometry and/or material properties of the membrane are altered.



## 5 Conclusions and Further Work

In this work, a behavioral model of an implantable device for ISR early detection has been presented. Test related problems for implantable capacitive MEMS pressure sensors have been considered; especially those cases which significantly affect the properties of the diaphragm. The deflection issue of circular membranes has been proved to be solvable for a fault-free case, using an accurate analytical behavioral model. Nevertheless, the aforementioned mathematical model evidences a lack of accuracy when tested under fault-injection conditions. The creation of additional models to precisely describe the behavior of a flexible diaphragm under faulty scenarios, using deflection results from FEA simulations, seems to be an essential requirement to completely characterize implantable MEMS pressure sensors.

**Acknowledgments.** This work was carried out in collaboration with the cardiology department of the University Hospital Marqués de Valdecilla, Santander (Spain). We would like to acknowledge the funding for this research from Ministerio de Ciencia e Innovación (Spain), Plan Nacional de I+D+i, project TEC2010-19122.

## References

1. OECD, Health at a Glance 2011: OECD Indicators, OECD Publishing, [http://www.oecd-ilibrary.org/social-issues-migration-health/health-at-a-glance\\_19991312](http://www.oecd-ilibrary.org/social-issues-migration-health/health-at-a-glance_19991312) (2011).
2. Hoffmann, R., Mintz, G.S.: Coronary in-stent restenosis - predictors, treatment and prevention. *European Heart Journal*, 21, pp. 1739-1749 (2000).
3. Takahata, K., Gianchandani, Y. B., Wise, K.D.: Micromachined Antenna Stents and Cuffs for Monitoring Intraluminal Pressure and Flow. *Journal of Microelectromechanical Systems*, 15(5), pp. 1289-1298 (2006).
4. Wang, M., Chen, J.: Volumetric Flow Measurement Using an Implantable CMUT Array. *IEEE Transactions on Biomedical Circuits and Systems*, 5(3), pp. 214-222 (2011).
5. Chow, E.Y., Chlebowski, A.L., Chakraborty, S., Chappell, W.J., Irazoqui, P.P.: Fully Wireless Implantable Cardiovascular Pressure Monitor Integrated with a Medical Stent. *IEEE Transactions on Biomedical Engineering*, 57(6), 1487-1496 (2010).
6. Zhao, W., Wang, C., Nakahira, Y.: Medical Application on Internet of Things. *Proceedings of IET International Conference on Communication Technology and Application (ICCTA 2011)*, pp. 660-665 (2011).
7. Young, D.F.: Some factors affecting pressure-flow relationships for arterial stenoses. *ASME Conf. Appl. Mech. Bioeng. Flu. Eng.*, pp. 87-90 (1983).
8. Marques, K.M.J.: Combined flow and pressure measurements in coronary artery disease. Amsterdam: Vrije Universiteit (2008)
9. Arfah, N., Alam, A.H.M.Z., Khan, S.: Capacitance-to-Voltage Converter for Capacitance Measuring System. 4th International Conference on Mechatronics (ICOM), pp. 1-4 (2011).
10. Rothman, A., Perry, S.B., Keane, J.F. and Lock, J.E.: Early results and follow-up of balloon angioplasty for branch pulmonary artery stenoses. *Journal of the American College of Cardiology*, 15(5), pp. 1109-1117 (1990).
11. Timoshenko S.: *Theory of Plates and Shells*. McGraw-Hill, New York (1940).
12. Landsberger L. M., Nashed S., Kahrizi M., Paranjape M.: On Hillocks Generated During Anisotropic Etching of Si in TMAH. *Journal of Microelectromechanical Systems*, vol. 5, no. 2, pp. 106-116 (1996).